THE ASTROPHYSICAL JOURNAL, 493:L63–L66, 1998 February 1
© 1998. The American Astronomical Society. All rights reserved. Printed in U.S.A.

MOLECULAR GAS IN THE INNER 100 PARSECS OF M51

N. Z. SCOVILLE,[1] M. S. YUN,[2] L. ARMUS,[1] AND H. FORD[3]
Received 1997 June 30; accepted 1997 November 20; published 1998 January 14

ABSTRACT

We report imaging of CO (2–1) emission in the nucleus of M51 at 1″ (47 pc) resolution. Molecular gas is found closely associated with the nuclear radio jet and the X-shaped dust absorption feature seen in the *Hubble Space Telescope* images. The CO emission lies along the side of the nuclear radio continuum "jet." The strongest molecular emission is not symmetric in either position or velocity with respect to the nucleus—the dominant feature is at redshifted velocities and peaks 1″ to the west of the radio/optical nucleus. The CO (2–1) emission has an integrated flux implying a molecular gas mass of $10^7\ M_\odot$ for a standard Galactic giant molecular cloud CO-to-H_2 conversion ratio, which is consistent with the total virial mass of the individual complexes. The redshifted CO emission is elongated with a deconvolved semimajor axis of 65 pc (1.″38). Assuming the molecular gas moves in circular orbit about the nucleus (defined by the point radio source), we find a dynamical mass of $2 \times 10^8\ M_\odot$ at $R \geq 47$ pc with no correction for inclination. The molecular gas has sufficient density ($\geq 10^5$ cm^{-3}) to collimate the radio jet and ionized outflow from the active galactic nucleus (AGN), and this gas may in fact be the reservoir of matter that supplies the AGN.

Subject heading: galaxies: individual (M51) — ISM: molecules

1. INTRODUCTION

The relationship of the central kiloparsec region in galaxies to the nuclear activity occurring on scales of ≤1–∼50 pc is likely to be critical to our understanding of the formation, evolution, and observed characteristics of active galactic nuclei (AGNs). In as much as the interstellar medium (ISM) has a high volume filling factor and is therefore much more dissipative than the stars, it is the most obvious source of accretion; in addition, the ISM will exhibit most strongly the effects of energy release from a central AGN.

M51 (NGC 5194) is one of the nearest galaxies with clear, albeit low-level, nuclear activity. In the nucleus, a point radio source is seen with a bipolar jet emerging at P.A. = −10° (Ford et al. 1985; Crane & van der Hulst 1992). Optical spectroscopy by Cecil (1988) shows narrow emission lines in two clouds or lobes aligned with the radio jet and extending out to 5″–10″ radius (Cecil 1988). At smaller scales, imaging with the *Hubble Space Telescope* (*HST*) has revealed X-shaped dust lanes, centered on the nucleus and extending to ∼1″ radius (Ford 1993; Grillmair et al. 1997). CO (1–0) and HCN (1–0) emission was mapped in the center of M51 by Kohno et al. (1996) and Helfer & Blitz (1997) at 4″ and 7″ resolution, respectively. Kohno et al. (1996) show the redshifted and blueshifted HCN emission straddling the radio jet axis at approximately the same P.A. as the more opaque arm of the "X." In this Letter, we report higher resolution (1″ corresponding to 47 pc; see Table 1) aperture synthesis observations in the CO (2–1) line to elucidate this molecular structure and to accurately measure the kinematics of the circumnuclear gas—hence placing dynamical constraints on the nuclear mass concentration.

2. OBSERVATIONS

The nucleus of M51 was observed using the Owens Valley Millimeter Array in the high-resolution configuration on 1996 December 26 and April 7. The array consists of six 10.4 m telescopes, and the baselines ranged from 35 to 242 m. The data were used only from this configuration in order to obtain the highest resolution and to provide a spatial filter against the much stronger, extended emission from the inner disk and spiral arms of M51 (cf. Rand & Kulkarni 1990; Aalto et al. 1997). Based on a comparison with the IRAM 30 m CO (2–1) data (S. Garcia-Burillo 1997, private communication), we estimate that our spectrum (see Fig. 1) recovers ∼50% of the total flux in the red wing but only 20% in the blue wing. The synthesized beams were 0.″74 × 1.″14 (uniform weighted) and 0.″76 × 1.″20 (natural), both at P.A. = −82° (see Table 1). The system temperatures were typically 800–900 K in the signal sideband, corrected for antenna and atmospheric losses and for atmospheric incoherence. Spectral resolution was provided by a digital correlator configured with 120 × 4 MHz channels (5.2 km s^{-1} resolution). The total usable integration time on M51 was 6.2 hr. The nearby quasar 1308+326 (1.9 Jy at 230 GHz) was used to track the phase and gain variations. The positional accuracy of the resulting maps is ∼0.″2. For the continuum maps (bandwidth = 1 GHz), the rms noise was 4.2 and 4.3 mJy for natural and uniform weighting, respectively. No continuum was detected, which is not surprising given the λ = 6 cm continuum fluxes: 0.6 mJy for the nuclear point source and a total 3 mJy within 8″ radius.

3. RESULTS

In Figure 1, the interferometric spectrum integrated over the 3″ region centered on the central radio point source at the nucleus of M51 is shown. The CO (2–1) emission inside 70 pc radius of the radio point-source nucleus is redshifted by about 60 km s^{-1} with respect to the systemic velocity (472 km s^{-1}); the peak CO (2–1) flux is 447 ± 23 mJy at 524 km s^{-1}, and the line width is 62 ± 10 km s^{-1} (FWHM).

In Figure 2, channel maps of the CO emission integrated over velocity ranges with $\Delta V = 20.8$ km s^{-1} (16 MHz) are shown. It is noteworthy that the CO (2–1) emission is seen mainly on the west of the nucleus and on the red side of the line, in contrast to the HCN emission reported by Kohno et al. (1996). As a check that the asymmetry seen in our data is real,

[1] California Institute of Technology, Pasadena, CA 91125.
[2] National Radio Astronomy Observatory, P.O. Box O, 1003 Lopezville Road, Socorro, NM 87801.
[3] Johns Hopkins University, Charles and 34th Street, Bloomberg Center, Baltimore, MD 21218.

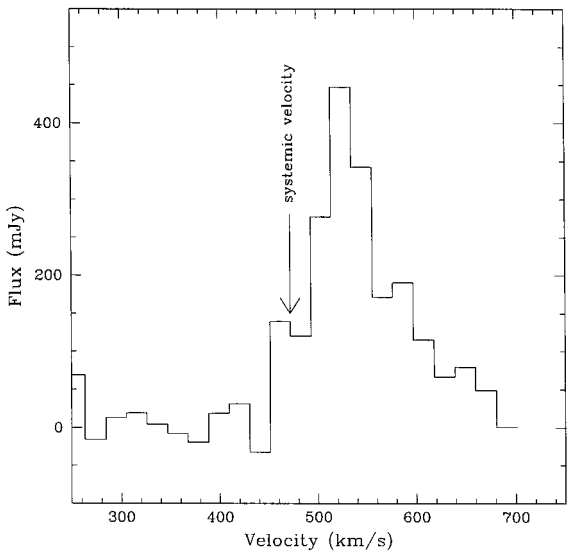

FIG. 1.—Spectrum of CO (2–1) emission in M51 smoothed to 16 MHz (20.8 km s^{-1}) resolution is shown for a 3″ (70 pc radius) aperture centered on the nuclear radio source in M51.

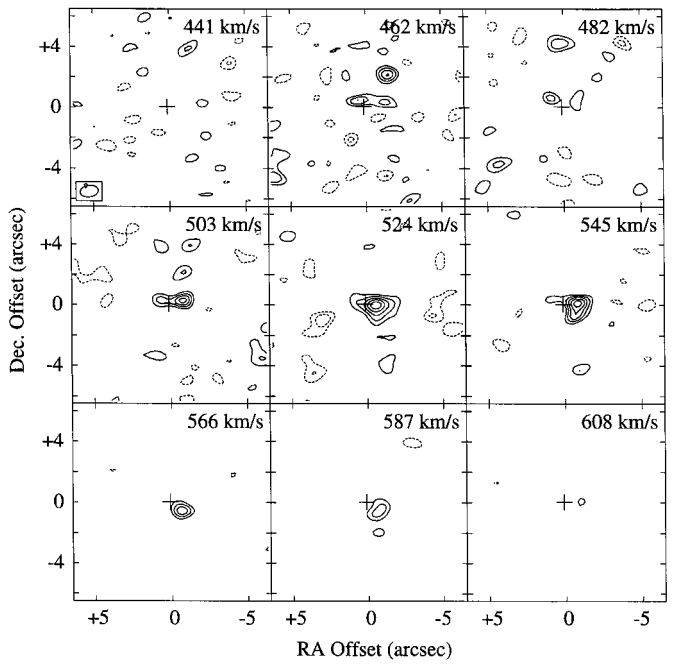

FIG. 2.—Maps of the CO (2–1) emission in M51 averaged over 20.8 km s^{-1} velocity ranges are shown as a function of coordinate offset from the nuclear point radio source (Crane & van der Hulst 1992; see Table 1). The LSR velocities of each channel are shown on the upper right-hand corner (the systemic velocity is 472 km s^{-1}). The contours are −3, −2, 2, 3, 4, 5, and 6 × 30 mJy $beam^{-1}$ (1 σ). (The higher noise at velocities close to systemic is due to the larger fraction of the emission being resolved out.)

we accessed CO (1–0) data at 2.″5 resolution obtained by Aalto et al. (1997) as part of a much larger mapping project for the inner disk of M51. The same asymmetries in both position and velocity are seen in the CO (1–0) line, and we are therefore confident that they are real. In addition, earlier low-resolution (4″) data obtained by us in the CO (2–1) line also show the asymmetries but are not included in the maps presented here because the data introduce aliasing from the more extended disk emission.

In Figure 3, the total CO line flux integrated over 224 MHz (291 km s^{-1}) centered on the line is shown superposed on the *HST* Hα-band image (Ford et al. 1997) and the 6 cm radio continuum (Crane & van der Hulst 1992). In both Figures 2 and 3, the maps are derived from naturally weighted *uv* data. The flux in the integrated CO map is 42 ± 4 Jy km s^{-1}. Five distinct CO features are identified in Figure 3, and the derived properties, including the deconvolved sizes, are summarized in Table 2. The brightest emission feature (S1 in Fig. 3) accounts for over 60% of all the mapped CO emission and has a deconvolved size of 1.″38 ± 0.″02 by 0.″54 ± 0.″02 (FWHM). The major-axis diameter corresponds to 65 pc, or a radius of 32 pc. The CO (2–1) emission is clearly resolved since the emission centroid shifts in the channel maps (see Fig. 2), with higher velocities in the line profile peaking to the south.

The peak flux in the narrowband channel maps (205 ± 30 mJy) implies a beam-averaged Rayleigh-Jeans brightness temperature excess of 5.1 K (9.6 K in Planck temperature) at $\lambda = 1.3$ mm. The peak brightness temperatures for all five CO complexes are similarly high (see Table 2), averaged over the 56 × 36 pc beam area. This suggests that the mean gas temperature is significantly higher than a typical Galactic plane giant molecular cloud (GMC; 5–10 K) since the observed brightness temperatures are undoubtedly affected by beam dilution. The true kinetic temperatures of the CO complexes are very likely more similar to the 25–100 K range seen in Galactic center GMCs. The gas density (n_{H_2}), obtained by dividing the masses by their volumes, ranges between 300 and 8000 cm^{-3}, averaged over the beam area.

TABLE 1

SUMMARY OF CO OBSERVATIONS AND DERIVED PROPERTIES

Parameter	Value
R.A. (B1950)[a]	$13^h27^m46^s33$
Decl. (B1950)[a]	+47°27′10″2
$\langle V \rangle_{LSR}$[b]	472 km s^{-1}
Adopted distance[c]	9.6 Mpc (1″ → 47 pc)
Adopted inclination[c]	20°
Major-axis P.A.[c]	170°
Synthesized beam (FWHM)	0.″76 × 1.″20 (P.A. = −82°) (36 × 56 pc)
M_{H_2} ($R < 70$ pc)[d]	7.7 × 10^6 $M_\odot$
$M_{dyn} \sin^2 i$ ($R < 70$ pc)	3 × 10^8 $M_\odot$

[a] Radio point source nucleus (Crane & van der Hulst 1992).
[b] CO systemic velocity (Scoville & Young 1983).
[c] Sandage & Tammann 1975 and Tully 1974.
[d] Using $\alpha = 4\ M_\odot$ (K km s^{-1} $pc^2)^{-1}$.

4. ANALYSIS AND DISCUSSION

From the integrated line flux of 42 ± 4 Jy km s^{-1}, we obtain a total CO (2–1) luminosity of $L'_{CO} = 2.7 \times 10^6$ K km s^{-1} pc^2. For a Galactic conversion factor $\alpha_{Gal} = 4\ M_\odot$ (K km s^{-1} $pc^2)^{-1}$, the total molecular mass is 1.1 × 10^7 $M_\odot$. It is of course possible that the Galactic CO-to-H_2 conversion factor is not appropriate to the molecular emission in M51. For low-excitation GMCs in the Galactic disk, the line temperature ratios are typically (1–0):(2–1):(3–2) = 1:0.7:0.4 (Sanders et al. 1997), while in the Galactic center, the ratios are higher but still less than unity. If the clouds are hotter or denser than Galactic GMCs, the conversion factor should vary as $n^{1/2}/T_{CO}$. To some extent, the decrease in the conversion factor due to the hotter gas in the circumnuclear region may be offset by increased density; for example, in Arp 220, a conversion factor

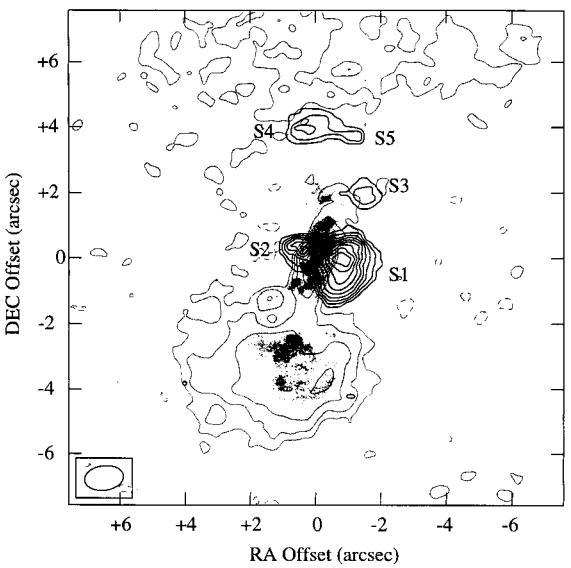

FIG. 3.—Integrated CO (2–1) emission (*heavy contours*) and the 6 cm radio continuum (*light contours*; Crane & van der Hulst 1992) are shown superposed on the *HST* Hα image (Ford et al. 1997). The CO emission was integrated over all channels containing significant line emission (V_{LSR} = 400–620 km s^{-1}), and the contours are 10% of the peak (15.6 Jy km s^{-1} beam^{-1}). Five distinct CO sources are identified in the map as S1–S5, and their properties summarized in Table 2. Three bright CO clouds are seen to the north of the nucleus outside 70 pc radius (1.″5).

of $0.45\alpha_{Gal}$ was derived from modeling of the CO line profiles and velocity field assuming that the dominant mass component was molecular gas (Scoville, Yun, & Bryant 1997). In the discussion below, we will use a molecular gas mass $1 \times 10^7\ M_\odot$ within 50 pc radius of the nucleus.

Based on the measured offsets and velocities of the CO emission, it is possible to estimate the dynamical mass interior to the CO emission feature. Assuming the gas is in circular orbit about the nucleus as defined by the position of the radio point source, $M_{dyn} = RV_{rot}^2/G \sin^2 i$. For V_{rot}, we adopt 135 km s^{-1}, i.e., nearly the maximum velocity offset from the systemic velocity of the CO emission on the red side of the line at $R = 47$ pc (1″). The mass interior to 47 pc is then $2 \times 10^8\ M_\odot$ (with no correction for inclination). We adopted the terminal red velocity as the rotation velocity rather than half the line width or the displacement of the peak velocity from the systemic velocity, since the center of mass in the nucleus is almost surely in the same rest frame as the galaxy as a whole and the lack of equivalently high velocity on the blue side of the line is very likely due simply to an absence of gas in the appropriate area of the nuclear disk. If the gas is orbiting in a plane with the same inclination as the inner disk of M51 ($i = 20°$; Tully 1974), the mass is increased by a factor of ~8. However, such a low inclination for the molecular gas seems inconsistent with the bipolar morphology of the radio jet and the optical emission-line outflow and the apparent interaction of the emission-line outflow with the M51 disk gas. With no correction for inclination, the molecular gas constitutes only 4% of the total dynamical mass (assuming the Galactic CO-to-H_2 conversion factor).

Kohno et al. (1996) imaged the HCN (1–0) line at 4″ resolution in the nucleus of M51. Their maps show much greater symmetry with respect to the nucleus: redshifted emission is seen on the west (consistent with our results), but almost equivalently strong blueshifted HCN emission is seen by them on the east. Some of this discrepancy could be due to the different spatial filtering of the different *u-v* sampling since neither data set includes all of the single-dish flux from the nucleus and, as noted earlier, our spectrum in Figure 1 recovers only 20%–50% at the different velocities. The unrecovered flux is presumably in a smooth, extended component. In our CO (2–1) maps, the blueshifted emission is about 4 times weaker than the redshifted emission. The reason for this discrepancy is unclear. Helfer & Blitz (1997) see only the redshifted HCN emission to the northwest of nucleus and do not see the blueshifted emission; yet both the signal-to-noise ratio and the resolution of their data are lower than those of Kohno et al. (1996). It is worthwhile noting that the CO (2–1) flux seen by us from the *blueshifted* region of the nucleus corresponds to a lower average brightness temperature than that of the HCN emission from the same location as reported by Kohno et al. (1996). In the blueshifted region of M51, the CO (2–1)/HCN (1–0) flux ratio would have to be ≤3 if the HCN fluxes given by Kohno et al. (1996) are compared with the CO (2–1) measured here. The case that comes closest to this is the nucleus of NGC 1068 where the flux ratios are CO (2–1)/CO (1–0) = 8 and CO

TABLE 2
PROPERTIES M51 CO COMPLEXES

Parameter	S1	S2	S3	S4	S5
α_{1950}	13 27 46.25	13 27 46.33	13 27 46.18	13 27 46.34	13 27 46.22
δ_{1950}	47 27 10.05	47 27 10.43	47 27 12.21	47 27 14.24	47 27 14.03
$\langle V_{CO} \rangle$ (km s^{-1})	545	503	462	472	492
ΔV_{FWHM} (km s^{-1})	73	105	<21	42	...
Deconvolved diameter:					
Arcseconds	1.38 × 0.54	<0.5	<0.5	0.82 × 0.29	<0.5
Parsecs	65 × 25	<23	<23	39 × 14	<23
P.A. (deg)	+172	...	...	+101	...
ΔT_{R-J} (K)	5.1	4.0	3.9	3.0	2.4
$S_{CO}\Delta V$ (Jy km s^{-1})	28.3	5.14	2.24	4.66	1.42
L'_{CO}[a]	16.3	2.94	1.29	2.67	0.82
M_{H_2} ($10^6\ M_\odot$)[b]	6.52	1.18	0.52	1.17	0.33
M_{vir} ($10^6\ M_\odot$)[b]	15.0	<16.0	<0.6	2.9	...

NOTE.—Units of right ascension are hours, minutes, and seconds, and units of declination are degrees, arcminutes, and arcseconds.

[a] In units of 10^5 K km s^{-1} pc^2.

[b] Using $\alpha = 4\ M_\odot$ (K km s^{-1} pc^2)$^{-1}$; virial mass $M_{vir} = 0.54r(\Delta V)^2/G$, where $r = 0.25\ (d_{maj} + d_{min})$.

(1–0)/HCN (1–0) = 3 (Baker & Scoville 1997), implying a flux ratio for CO (2–1)/HCN (1–0) = 24.

The location of the CO emission along the western side of the radio jet is suggestive that the dense molecular gas may collimate the jet along an axis perpendicular to the orbital plane of the molecules. Similarly, it may confine the high-velocity gas seen in the optical emission line outflow to the same axis. The pressure of the radio jet is $\sim 10^{-9}$ dyn cm^{-2} (Crane & van der Hulst 1992); for molecular gas at 100 K, the density required for its thermal pressure to be in equilibrium with the radio jets is $\sim 10^5$ cm^{-3} (and an even much lower density is required if the equilibrium is with the cloud internal turbulent pressure). This density is consistent with the value of $\sim 10^5$ cm^{-3} recently derived from analysis of HCN, ^{13}CO, and CO (1–0) emissions by Matsushita et al. (1997). The high densities can also be inferred from the masses we derive individually for the molecular complexes S1 and S2 (Table 2). Given the high density and resulting high pressure of molecular gas and its distribution observed here, it is likely that the axes of the radio jet and the ionized gas outflow (P.A. = -10°) are determined by the orbital plane of the dense interstellar medium rather than a preferred axis within the AGN. Asymmetries in molecular gas distribution may then account for the quite different morphologies of the radio jets to the north and south of the nucleus as speculated by Crane & van der Hulst (1992).

The high density of the gas seen in the nuclei of galaxies like M51 is not surprising; it is, in fact, probably an inevitable consequence of the requirement that the density be sufficient to bind against tidal shear. Scaling to the dynamical mass obtained above for M51 at 50 pc radius, the condition for tidal stability of the gas is

$$n_{\mathrm{H_2}} \sim 2 \times 10^4 \ \mathrm{cm^{-3}} \left(\frac{M_{\mathrm{dyn}}}{2 \times 10^8 \ M_\odot}\right)\left(\frac{R}{50 \ \mathrm{pc}}\right)^{-3}. \quad (1)$$

If the gas mass ($1 \times 10^7 \ M_\odot$) estimated earlier is uniformly distributed over a sphere of radius 50 pc, the mean density is only $n_{\mathrm{H_2}} = 400$ cm^{-3}. Thus, in order to withstand tidal stresses, in the absence of a confining pressure, the gas must be either clumped or confined to a thin, dense disk. In the former case, the clumps would fill 2% of the volume; in the latter, the disk must have a mean thickness of $\sim$10 pc if its area is $\sim$50% covered. (Pressure confinement of observed velocity dispersions of the molecular complexes [i.e., their internal supersonic turbulence] would require a pressure in the nucleus approximately 10^4 times greater than that of the radio jet estimated by Crane & van der Hulst (1992). Since the radio jets are clearly not totally suppressed, this in fact provides a strong argument against there being a high intercloud pressure.) In any case, even if the gas is clumped in discrete, high density clouds rather than a smooth disk, it is likely that these clouds are confined to a disk since the gas on opposite side of the nucleus is at opposing velocities with respect to systemic and the gas distribution is elongated along the same axis.

An interesting comparison may be made between the central 100 pc of M51 and the area surrounding Sgr A*, the central source in our Galaxy. The gaseous environment of Sgr A* can be described as a 2 pc molecular circumnuclear ring straddled by two massive ($\gtrsim 3 \times 10^5 \ M_\odot$) giant molecular clouds located at about 10 pc radius (Armstrong & Barrett 1984; Ho et al. 1985; Gusten et al. 1987). Such massive molecular clouds located 10 pc radius from the central potential must also have a high density in order to survive tidal disruption (Scoville, Solomon, & Thaddeus 1972; Ho et al. 1985). Inside the 2 pc circumnuclear ring surrounding Sgr A*, the gas appears largely ionized and as dense ionized spiral-like streamers, which are perhaps material falling onto the central source, Sgr A* (Lo & Claussen 1983; Ho et al. 1991). At the distance of M51, only the two massive GMCs at 10 pc radius would be detectable with the 1″ resolution observations presented here. The X-shaped dust lanes and ionized structures seen with the *HST* may be the scaled-up counterparts of the 2 pc circumnuclear ring and inner spiral in our Galactic center.

In conclusion, we have found strong evidence for the existence of dense molecular gas in the central $\lesssim$50 pc of M51. This gas is probably confined to a disk and has sufficient density ($\gtrsim 10^5$ cm^{-3}) to collimate the jet and ionized outflow from the AGN. Although we have not estimated the radial accretion rate in the molecular gas since the velocity dispersion and non-axisymmetries in the potential are currently undetermined, the observed molecular gas certainly has sufficient mass to be considered as a possible reservoir of matter to feed the AGN.

The Owens Valley millimeter array is supported by NSF grants AST 93-14079 and AST 96-13717. N. Scoville thanks Dave Sanders for hospitality at the Institute for Astronomy, University of Hawaii, where part of this work was done. We also thank the referee, T. Helfer, for constructive advice and S. Aalto-Bergman and S. Huetemeister for sharing their CO (1−0) data with us. E. de Geus helped with early phases of this work, and Z. Tsvetanov provided the *HST* image for Figure 3.

REFERENCES

Aalto-Bergman, S., Huetemeister, S., Scoville, N. Z., & Thaddeus, P. 1997, in preparation
Armstrong, J. T., & Barrett, A. H. 1984, ApJS, 57, 535
Baker, A. J., & Scoville, N. Z. 1997, in preparation
Cecil, G. 1988, AJ, 392, 38
Crane, P. C., & van der Hulst, J. M. 1992, AJ, 103, 1146
Ford, H. C. 1993, NASA Press Release, ST Sci-PRC92-17
Ford, H. C., Crane, P. C., Jacoby, G. H., Lawrie, D. G., & van der Hulst, J. M. 1985, ApJ, 293, 132
Ford, H. C., et al. 1997, in preparation
Grillmair, C. J., Faber, S. M., Lauer, T. R., Hester, J. J., Lynds, C. R., O'Neil, E. J., & Scowen, P. A. 1997, AJ, 113, 225
Gusten, R., Genzel, R., Wright, M. C. H., Jaffe, D. T., Stutzki, J., & Harris, A. I. 1987, ApJ, 318, 124
Helfer, T. T., & Blitz, L. 1997, ApJ, 478, 162
Ho, P. T. P., Ho, L. C., Szczepanski, J. C., Jackson, J. M., Armstrong, J. T., & Barrett, A. H. 1991, Nature, 350, 309
Ho, P. T. P., Jackson, J. M., Barrett, A. H., & Armstrong, J. T. 1985, ApJ, 288, 575
Kohno, K., Kawabe, R., Tosaki, T., & Okimura, S. K. 1996, ApJ, 461, L29
Lo, K. Y., & Claussen, M. 1983, Nature, 306, 647
Matsushita, S., Kohno, K., Vila-Vilaro, B., Tosaki, T., & Kawabe, R. 1997, preprint
Rand, R. J., & Kulkarni, S. R. 1990, ApJ, 349, L43
Sandage, A., & Tammann, G. A. 1975, ApJ, 196, 313
Sanders, D. B., Carpenter, J., Tilanus, R., Deane, J., & Scoville, N. 1997, in preparation
Scoville, N. Z., Solomon, P. M., & Thaddeus, P. 1972, ApJ, 172, 335
Scoville, N. Z., & Young, J. Y. 1983, ApJ, 265, 148
Scoville, N. Z., Yun, M. S., & Bryant, P. M. 1997, ApJ, 484, 702
Tully, R. B. 1974, ApJS, 27, 437